ENGINEERING IN ADVANCED RESEARCH SCIENCE AND TECHNOLOGY

ISSN 2386-7876
Vol.01, Issue.03
March-2026
Pages: 430-439

A Low Complexity Data Detection Algorithm for Uplink Multiuser Massive MIMO Systems

[1] **Jyothirmai Kanchanapally**, [2] **Mogili Swathi**, [3] **Jogi Deepika**, [4] **Yerramsetti Anu Suresh**, [5] **Koruprolu Sai Manoj Kumar**

[1]M.tech,Assistant Professor, Dept of E.C.E, BVCITS, Batlapalem, Amalapuram, AP
[2,3,4,5]B. Tech, Dept of E.C.E, BVCITS, Batlapalem, Amalapuram, AP

ABSTRACT: Massive Multiple-Input Multiple-Output (massive MIMO) system relies on channel state information (CSI) feedback to perform precoding and achieve performance gain in frequency division duplex (FDD) networks. However, transmission of massive MIMO system is subject to excessive feedback overhead. To improve the channel estimation performance, we propose a prior-aided Gaussian mixture LAMP (GM-LAMP) based beam space channel estimation scheme in this paper. Specifically, based on the prior information that beam-space channel elements can be modeled by the Gaussian mixture distribution, we first derive a new shrinkage function to refine the AMP algorithm. Then, by replacing the original shrinkage function in the LAMP network with the derived Gaussian mixture shrinkage function, a prior-aided GM-LAMP network is developed to estimate the beam space channel more accurately. Simulation results by using both the theoretical channel model and the ray-tracing based channel dataset show that, the proposed GMLAMP network can achieve better channel estimation accuracy.

Keywords: Multiple input Multiple Output, channel state information, frequency division duplex, Gaussian mixture.

INTRODUCTION: The fifth generation (5G) wireless communications networks have a lot of novel requirements, such as the high system capacity with respect to the fourth generation (4G) networks, wide frequency range (Covering through millimeter wave (mmWave) bands), increased data rate, ultra-low latency, reduced energy, and low cost [1]. Massive MIMO system was found very promising to be utilized in 5G systems to achieve its requirements. In addition, using massive MIMO systems brought new challenges on channel modeling [2]. It is quite notable that one of the performance bounds of 5G, like any other communication system, is determined by channel characteristics. Therefore, an accurate channel model plays an important role in designing, evaluating, and developing wireless communication systems. Massive MIMO channel state information (CSI) feedback techniques were devised in order to get more accurate and dynamic estimate of channel parameters, as compared with other channel models such as ITU-R IMT-2020, COST 2100 and the IEEE 802.11 ay models [3]. Artificial intelligence (AI) approaches were investigated in 5G systems to facilitate processing the signal received by massive MIMO antennas for the purpose of acquiring accurate channel estimation [4]. In this respect, a number of deep learning methods were proposed, with a variety of adopted algorithms. Compressive Sensing (CS) using the spatial and temporal correlation of CSI was used to obtain channel information with acceptable accuracy under substantially reduced feedback load [5]. Least Absolute Shrinkage and Selection Operator (LASSO) L1-solver [6] and Approximate Message Passing (AMP) [7], were used CS to estimate channel parameters. In [8], the authors utilized deep learning technology in massive MIMO to develop a CSI system, which was based upon using sensing and recovery network. The proposed network estimated the channel structure from training samples, and was called (CsiNet). In addition, several algorithms using Auto-encoder CsiNet arrangement which utilized few neural network (NN) layers were proposed in order to reduce the channel state information (CSI) feedback and perform recovery with high degree of accuracy [9]. The authors in [10] adopted a simple and efficient approach to reduce the overhead of downlink channel estimation and feedback using linear regression (LR) and support vector regression (SVR) in machine learning. Channel estimation is very challenging when the receiver is equipped with a limited number of radio-frequency (RF) chains in beam space millimeter-wave massive MIMO [11].

MIMO-OFDM IN LINEAR TIME-VARYING CHANNELS:

For MIMO-OFDM, denote the number of transmitters and receivers to be M and N, and the OFDM symbol length to be K. Denote the l-th channel tap between the m-th
transmitter and the n-th receiver at time slot t by

$h(t)\ l,m,n$, $l = 0, 1, \ldots, L-1$, where L is the channel length. Therefore, for linear time-varying channel model in one frame,

$h(t)\ l,m,n = hl,m,n+\delta t-l\alpha l,m,n$,

where $hl,m,n = 1K\ \_l+K-1\ t=l\ h(t)\ l,m,n$ is the time invariant part and
$\alpha l,m,n$ is the time-varying factor of its l-th channel tap.

$\delta i = iK - K-1\ 2K$ indicates the time varying step.

In [18] and [19], the input-output relationship of SISO-OFDM in linear time-varying channels has been introduced. For MIMO-OFDM, by regarding each pair of transmitter m and receiver n as a SISO-OFDM link, and by similar approach in [18] and [19], the time domain signal received at the *nth* receiver from the *mth* transmitter could be represented as

$\mathbf{y}m,n = (Hm,n + Am,nB)\mathbf{x}m$

where $\mathbf{x}m$ is the time domain sequence transmitted from the m-th transmitter, Hm,n is a $K \times K$ circulant matrix with the first column to be $[h0,m,n,\ h1,m,n,\ \cdots,\ hL-1,m,n,\ 0,\ \cdots,\ 0]T$, Am,n is a $K \times K$ circulant matrix with the first column to be $[\alpha 0,m,n,\ \alpha 1,m,n,\ \cdots,\ \alpha L-1,m,n,\ 0,\ \cdots,\ 0]T$, B is a diagonal matrix such that $B = Diag([\delta 0,\ \delta 1,\ \ldots,\ \delta K-1]T)$. Convert the signals to frequency domain,

MILLIMETER-WAVE (MMWAVE) COMMUNICATION IN MIMO:

Millimeter-wave (mmWave) communication [2], [3] and massive multiuser (MU) multiple-input multiple-output (MIMO) [4], [5] are expected to be core technologies of nextgeneration wireless communication systems. By combining both of these technologies, one can achieve unprecedentedly high-bandwidth data transmission to multiple user equipments (UEs) in the same time-frequency resource via fine-grained beamforming. The strong path loss of wave propagation at mmWave frequencies necessitates the infrastructure basestations (BSs) to acquire accurate channel state information (CSI) in order to perform data detection in the uplink (UEs transmit to BS) and MU precoding in the downlink (BS transmits to UEs) [6], [7]. To optimally determine the beamforming weights, accurate CSI is not only of paramount importance for hybrid analog-digital BS architectures [8]–[10] but also for emerging all-digital BS architectures [11], [12]. In addition, the trend towards BS architectures with low-precision data converters to reduce power consumption, interconnect bandwidth, and system costs [13]–[15] requires novel algorithms and hardware designs that denoise the estimated channel vectors.

CHANNEL ESTIMATION:

Fortunately, wave propagation at mmWave frequencies is predominantly directional and real-world channels typically comprise only a small number of strong propagation paths, such as a line-of-sight (LoS) component and a few first-order reflections [16]. These properties enable the design of sparsityexploiting CSI estimation algorithms that effectively suppress channel estimation errors [7]–[2]. Compressive sensing (CS)- based methods have been proposed for mmWave channel estimation in [21], [22], including methods that rely upon orthogonal matching pursuit (OMP) [2]–[4]. The majority of such methods uses a discretization procedure of the number of propagation paths that can be resolved in the beamspace (or angular) domain [5], which results in a problem widely known as basis mismatch [6]. To avoid the basis mismatch problem, sparse channel estimation for mmWave channels can, for example, be accomplished with atomic norm minimization (ANM) [7], [8] or Newtonized OMP [9].

ANM estimates a discrete set of propagation paths off-the-grid by solving a semidefinite program (SDP). Newtonized OMP (NOMP) is a more efficient alternative to ANM and iteratively refines the incident angles of the dominant propagation paths off-the-grid with a complexity only slightly higher than that of conventional OMP. Although both of these methods do not suffer from the basis mismatch problem and exhibit excellent denoising performance, they entail high computational complexity. Hence, from a hardware-implementation perspective, such methods are less attractive, especially in massive MU-MIMO systems where the complexity is dominated by the large number of BS antennas. In addition, the performance of both of these methods strongly depends on algorithm parameters that need to be tuned for the given propagation conditions. Another strain of sparsity-exploiting channel-estimation methods build upon approximate message passing (AMP) While such methods promise high estimation accuracy, they suffer from a number of drawbacks when implemented in VLSI.

EXISTING METHOD:

AMP algorithm and LAMP network:

Since the number of antennas in mmWave massive MIMO systems is usually large, the dimension of the sparse signal in (12) is high. Thanks to faster convergence, the iterative AMP algorithm can be used to recover the sparse signal with low computational complexity, especially for the highdimensional sparse signal [15]. In this subsection, we introduce how the complex-valued AMP algorithm estimates the beam space channel, as shown in Algorithm 1

Algorithm 1: Approximate Message Passing (AMP)

Input: The measurement vector $\mathbf{y}$, the sensing matrix $\mathbf{A}$, the number of iterations T.

Initialization: $\mathbf{v}_{-1} = \mathbf{0}, b_0 = 0, c_0 = 0, \hat{\tilde{\mathbf{h}}}_0 = \mathbf{0}$.

for $t = 0, 1, \cdots, T-1$ **do**

1. $\mathbf{v}_t = \mathbf{y} - \mathbf{A}\hat{\tilde{\mathbf{h}}}_t + b_t \mathbf{v}_{t-1} + c_t \mathbf{v}_{t-1}^*$
2. $\sigma_t^2 = \frac{1}{M} \|\mathbf{v}_t\|_2^2$
3. $\mathbf{r}_t = \hat{\tilde{\mathbf{h}}}_t + \mathbf{A}^T \mathbf{v}_t$
4. $\hat{\tilde{\mathbf{h}}}_{t+1} = \eta_{\mathrm{st}}(\mathbf{r}_t; \lambda_t, \sigma_t^2)$
5. $b_{t+1} = \frac{1}{M} \sum_{i=1}^{N} \frac{\partial \eta_{\mathrm{st}}(r_{t,i}; \lambda_t, \sigma_t^2)}{\partial r_{t,i}}$
6. $c_{t+1} = \frac{1}{M} \sum_{i=1}^{N} \frac{\partial \eta_{\mathrm{st}}(r_{t,i}; \lambda_t, \sigma_t^2)}{\partial r_{t,i}^*}$

end for

Output: Sparse signal recovery results: $\hat{\tilde{\mathbf{h}}} = \hat{\tilde{\mathbf{h}}}_T$.

In Algorithm 1, the term btvt−1 and term ctv ∗ t−1 in Step 1 are called Onsager Correction [15], which are introduced into the AMP algorithm to accelerate the convergence. The

critical step of the AMP algorithm is Step 4, in which the estimate h ˆ˜ t+1 in the tth iteration is obtained through the soft threshold shrinkage function ηst: C N → C N . The shrinkage function ηst is nonlinear element-wise operation, which takes the sparsity of the vector h˜ into consideration, and makes the estimate h ˆ˜ t+1 sparser. For the ith element rt,i = |rt,i| e jωt,i (i = 1, 2, · · · , N) of input vector rt, we have

$$\begin{aligned}\left[\eta_{\mathrm{st}}\left(\mathbf{r}_t; \lambda_t, \sigma_t^2\right)\right]_i &= \eta_{\mathrm{st}}\left(|r_{t,i}| e^{j\omega_{t,i}}; \lambda_t, \sigma_t^2\right) \\ &= \max\left(|r_{t,i}| - \lambda_t \sigma_t, 0\right) e^{j\omega_{t,i}},\end{aligned} \tag{13}$$

where ωt,i is the phase of complex-valued element rt,i, λt is the predefined and fixed parameter in the tth iteration, and σ 2 t is updated via estimating the noise variance in Step 2. From (13), we can find that the soft threshold shrinkage function ηst can shrink the amplitude of complex-valued input with low power to zero. In Step 5 and Step 6, the element-wise derivatives of the shrinkage function ηst at the input vector r and its conjure vector r ∗ are respectively calculated to obtain bt+1 and ct+1. Although the AMP algorithm is good at dealing with the large-scale sparse signal recovery problem, there are still two problems when it is used for the sparse beamspace channel estimation. First, the shrinkage parameter λt in (13) usually takes the same empirical value for all iterations. Second, the general AMP algorithm cannot fully exploit the prior distribution of the beamspace channel.

OPOSED METHOD:

GM-LAMP network

In order to estimate the beamspace channel more accurately, we integrate the LAMP network and the new shrinkage function derived from the Gaussian mixture distribution to propose a prior-aided GM-LAMP network. Specifically, we replace the original soft threshold shrinkage function in the existing LAMP network by the Gaussian mixture shrinkage function. Therefore, the proposed GM-LAMP network is still constructed on the AMP algorithm. Similar to Fig. 2, the GM-LAMP network also have T homogeneous

layers, where the inputs and outputs of each layer are the same as those of the LAMP network. The inputs of the tth layer are represented by y ∈ CM, h ˆ˜ t ∈ C N and vt ∈ CM, where y is the measurement vector, h ˆ˜ t and vt are the outputs of the (t − 1)th layer. The outputs of the tth layer can be represented by h ˆ˜ t+1 and vt+1, representing the estimate vector and residual vector of the tth layer, respectively. The difference is that the soft threshold shrinkage function ηst of each layer is replaced by the Gaussian mixture shrinkage function ηgm. To do this, the channel estimate h ˆ˜ t+1 of the tth layer in the GM-LAMP network can be obtained by

$$\mathbf{r}_t = \hat{\tilde{\mathbf{h}}}_t + \mathbf{B}_t \mathbf{v}_t, \quad (28)$$

$$\hat{\tilde{\mathbf{h}}}_{t+1} = \boldsymbol{\eta}_{\mathrm{gm}}\left(\mathbf{r}_t; \boldsymbol{\theta}_t, \sigma^2\right), \quad (29)$$

where σ 2 = ‖vt‖ 2 2 M is obtained in the same way as the AMP algorithm and the LAMP network [29], the linear transform coefficients Bt and nonlinear shrinkage parameters θt are trainable variables to be optimized in the training phase. Next, we discuss how the GM-LAMP network works for the beamspace channel estimation problem in mmWave massive MIMO systems. Like most existing DNNs [24]–[26], the GMLAMP network mainly works in two phases: offline training phase and online estimation phase. In the offline training phase, given a large number of known training data, the GMLAMP network aims to optimize overall trainable variables ΩT −1 = {Bt, θt} T −1 t=0 by minimizing the loss function. In the online estimation phase, by inputting the new measurements y, the trained GM-LAMP network can output the estimated beamspace channel h ˆ˜. Next, we introduce these two phases in detail.

1) **OFFLINE TRAINING PHASE**:

In this paper, we adopt the supervised learning to train the GM-LAMP network. The training dataset can be represented {y d , h˜d} D d=1, where y d is the input of the GM-LAMP network, h˜d is the corresponding label, and D represents the number of the training data. In order to avoid overfitting, the layer-by-layer training method adopted by [29] is used to train the GM-LAMP network. Generally speaking, the layer-by-layer training method can be explained from three steps. Firstly, the whole training procedure can be divided into T sequential training sub-procedures [29]. For the tth training sub-procedure, we aim to refine the trainable variables Ωt = {Bi , θi} t i=0 of the i = 0, · · · , i = tth layer. Each layer of the GM-LAMP network has its own loss functions. Secondly, we define two types of loss functions as follows, which are related to the linear transform operation and the nonlinear shrinkage operation:

$$L_t^{\mathrm{linear}}(\boldsymbol{\Omega}_t) = \frac{1}{D}\sum_{d=1}^{D}\left\|\mathbf{r}_t^d(\mathbf{y}^d, \boldsymbol{\Omega}_t) - \tilde{\mathbf{h}}^d\right\|_2^2, \quad (30)$$

$$L_t^{\mathrm{nonlinear}}(\boldsymbol{\Omega}_t) = \frac{1}{D}\sum_{d=1}^{D}\left\|\hat{\tilde{\mathbf{h}}}_{t+1}^{d}(\mathbf{y}^d, \boldsymbol{\Omega}_t) - \tilde{\mathbf{h}}^d\right\|_2^2, \quad (31)$$

where r d t is the output of the linear transform operation in (2), and h ˆ˜ d t+1 is the output of the nonlinear shrinkage operation in (i.e., the estimated channel of the tth layer). Based on these two loss functions, the training sub-procedure for the tth layer are further divided into the two parts: the linear training for aiming to minimizing L linear t and the nonlinear training for aiming to minimizing L nonlinear t . Thirdly, the hybrid method of "individual" and "joint" optimization is further adopted in linear training and the nonlinear training. Specifically, in the linear training of the tth training sub-procedure, only the linear transform coefficients Bt are first optimized individually, and all trainable variables Ωt−1 of the previous i = 0, · · · , i = (t − 1)th layer together with Bt are optimized jointly. Similarly, in the nonlinear training of the tth training sub-procedure, the nonlinear shrinkage parameters θt are first optimized individually, and then all trainable variables Ωt−1 of the previous i = 0, · · · , i = (t − 1)th layer together with Bt and θt are optimized jointly. Based on the above three steps, the trained GMLAMP network can be efficiently fine-tuned in each layer, and therefore avoid bad local optimum caused by overfitting

Algorithm 2: Layer-by-Layer Training Method

Initialization: $\mathbf{B}_0 = \boldsymbol{A}^T, \boldsymbol{\theta}_0 = \boldsymbol{\theta}^0$.

1. Learn $\mathbf{B}_0$ to minimize L_0^{linear}
2. Learn $\boldsymbol{\theta}_0$ with fixed $\mathbf{B}_0$ to minimize $L_0^{\mathrm{nonlinear}}$
3. Re-learn $\boldsymbol{\Omega}_0 = \{\mathbf{B}_0, \boldsymbol{\theta}_0\}$ to minimize $L_0^{\mathrm{nonlinear}}$

for $t = 1, \cdots, T-1$ **do**

4. Initialization: $\mathbf{B}_t = \mathbf{B}_{t-1}, \boldsymbol{\theta}_t = \boldsymbol{\theta}_{t-1}$
5. Learn $\mathbf{B}_t$ with fixed $\boldsymbol{\Omega}_{t-1}$ to minimize L_t^{linear}
6. Re-learn $\{\boldsymbol{\Omega}_{t-1}, \mathbf{B}_t\}$ to minimize L_t^{linear}
7. Learn $\boldsymbol{\theta}_t$ with fixed $\{\boldsymbol{\Omega}_{t-1}, \mathbf{B}_t\}$ to minimize $L_t^{\mathrm{nonlinear}}$
8. Re-learn $\boldsymbol{\Omega}_t = \{\boldsymbol{\Omega}_{t-1}, \mathbf{B}_t, \boldsymbol{\theta}_t\}$ to minimize $L_t^{\mathrm{nonlinear}}$

end for

Output: $\boldsymbol{\Omega}_{T-1}$.

Algorithm 2 shows the specific layer-by-layer training method. Steps 1-3 represent the training sub-procedure for the initial layer (i.e., t = 0), where B0 and θ0 are first optimized individually and then optimized jointly. Then, the training sub procedure for the t = 1, t = 2, · · · , t = (T − 1)th layer are performed sequentially. Before training, trainable variables of the tth layer are initialized as the values for those of the (t − 1)th layer, as shown in Step 4. Steps 5-6 and Steps 7- 8 represent the linear training and the nonlinear training of the training sub-procedure for the tth layer, respectively. Step 5 represents the individual optimization of linear transform coefficients Bt, while Step 6 represents the joint optimization of Ωt−1 and Bt. Similarly, Step 7 represents the individual optimization of nonlinear shrinkage parameters θt, while Step 8 represents the joint optimization of Ωt−1, Bt and θt. After overall trainable variables ΩT −1 of T layers are optimized, we can obtain a trained GM-LAMP network to directly estimate the beamspace channel.
2) Online estimation phase: In this phase, we apply the trained GM-LAMP network to the beamspace channel estimation problem in mmWave massive MIMO systems, where
he new measurements are fed into the trained GM-LAMP network to directly generate the corresponding estimates. Finally, the normalized mean square error (NMSE) is used to evaluate the performance of the GM-LAMP network:

$$\mathrm{NMSE} = \frac{\mathbb{E}\left\{\sum_{k=1}^{K}\left\|\hat{\tilde{\mathbf{h}}}_k - \tilde{\mathbf{h}}_k\right\|_2^2\right\}}{\mathbb{E}\left\{\sum_{k=1}^{K}\left\|\tilde{\mathbf{h}}_k\right\|_2^2\right\}}. \qquad (32)$$

RESULTS:

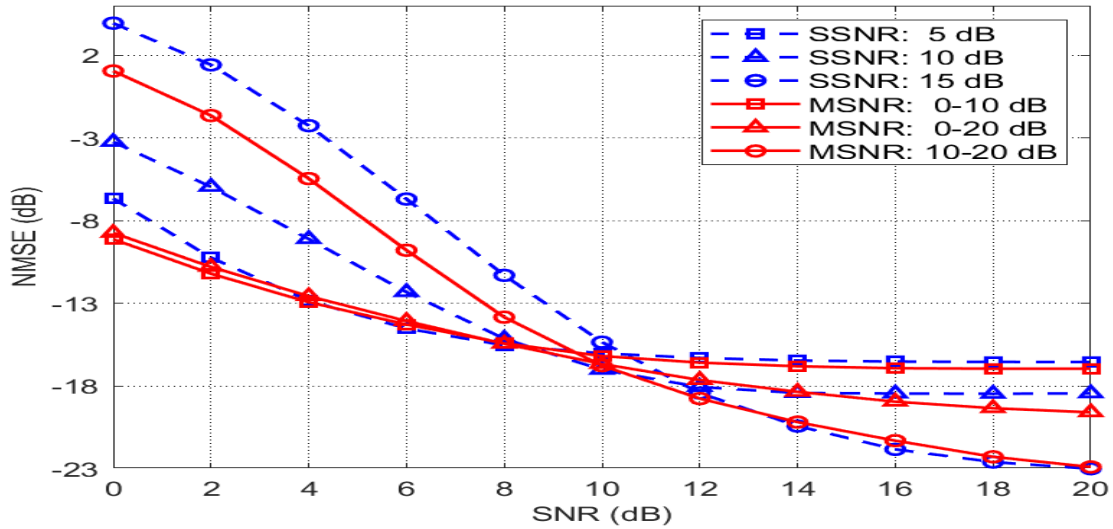

Fig:a NMSE performance comparison of different trained GM-LAMP networks with different training settings.

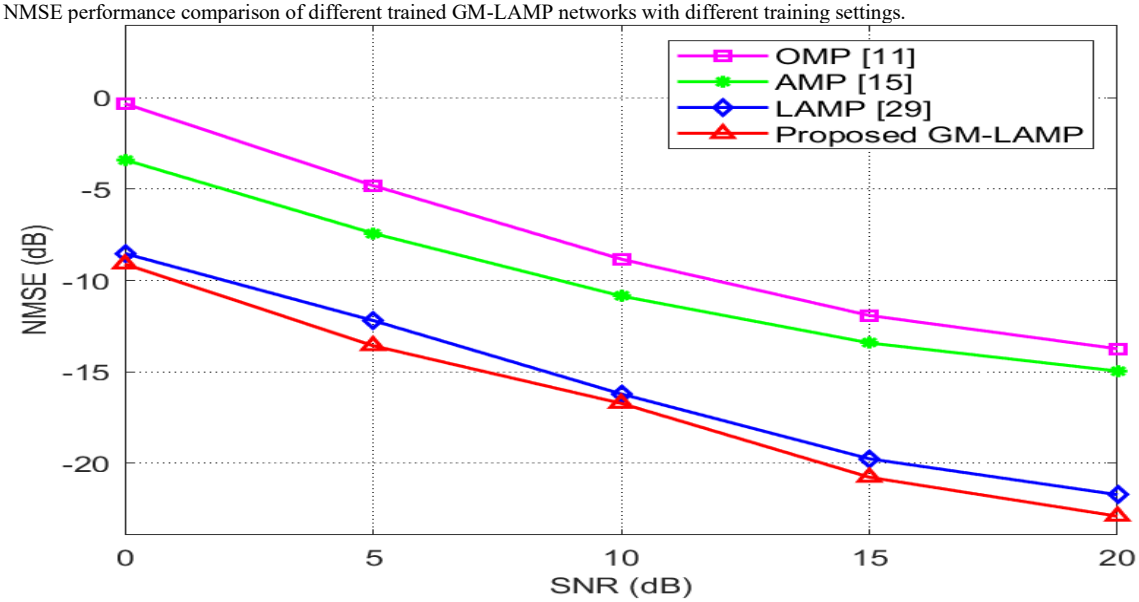

Fig: b NMSE performance comparison for ULAs based on the Saleh Valenzuela channel model.

NMSE performance comparison for ULAs based on the SalehValenzuela channel model.

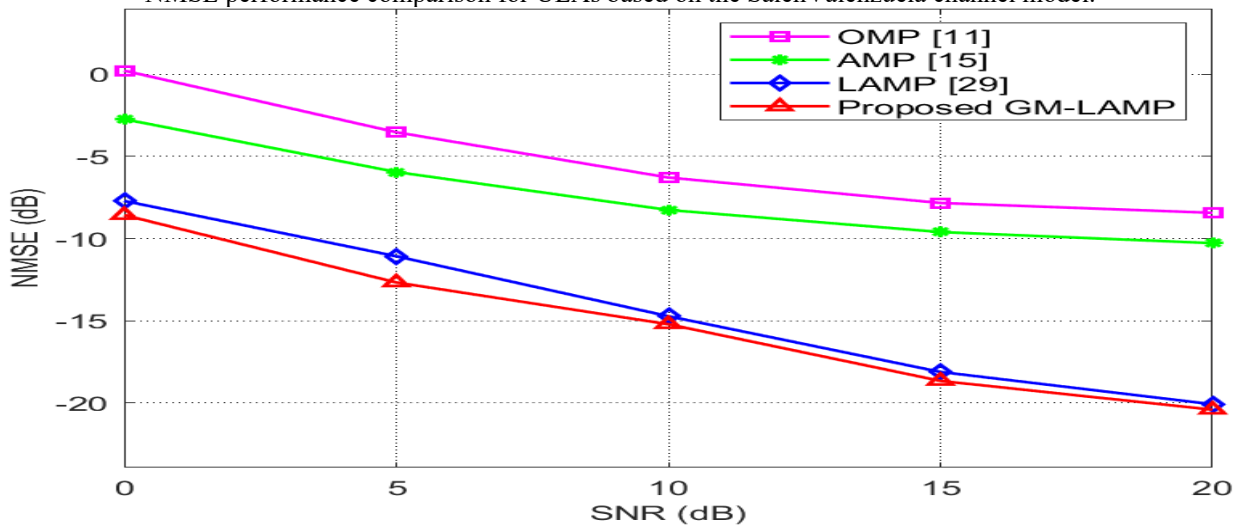

Fig. c NMSE performance comparison for UPAs based on the SalehValenzuela channel model.

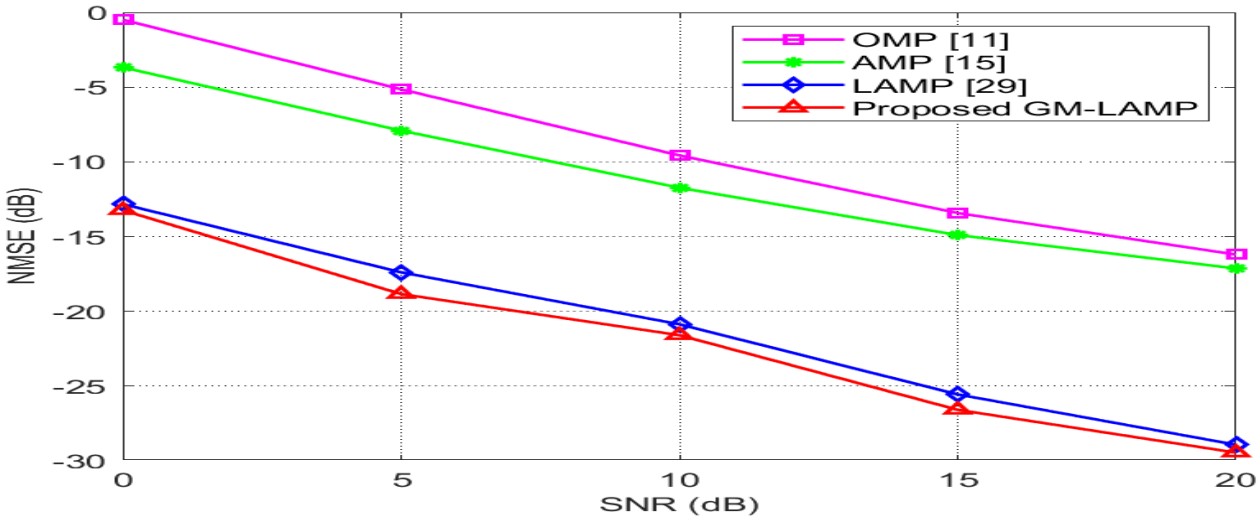

Fig: d NMSE performance comparison for ULAs based on the Deep MIMO dataset.

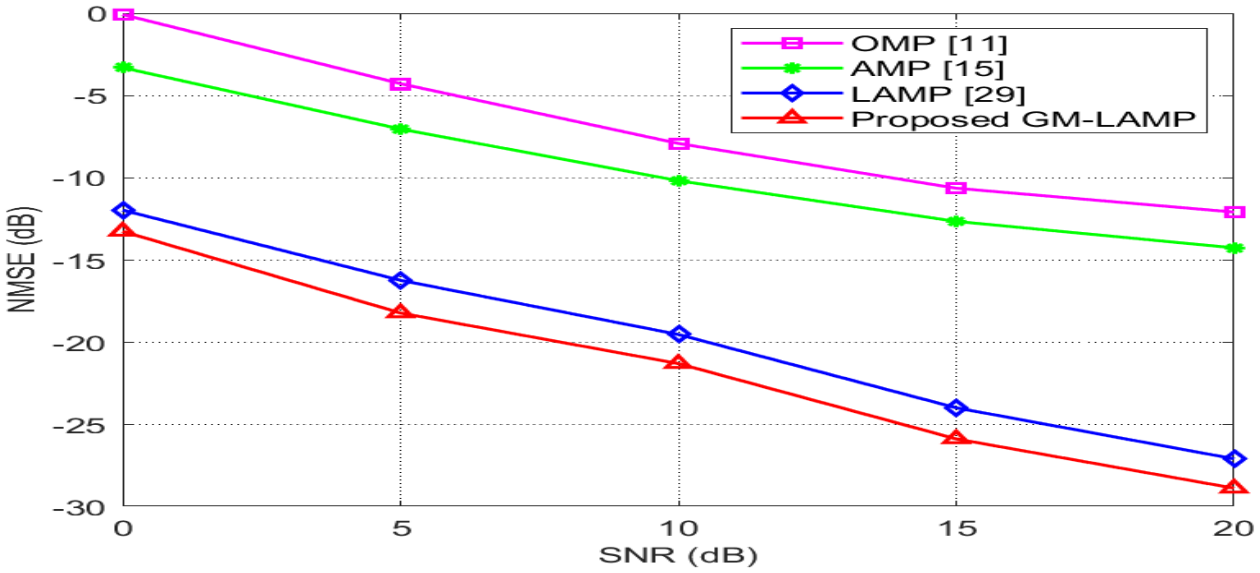

Fig: e NMSE performance comparison for UPAs based on the Deep MIMO dataset.

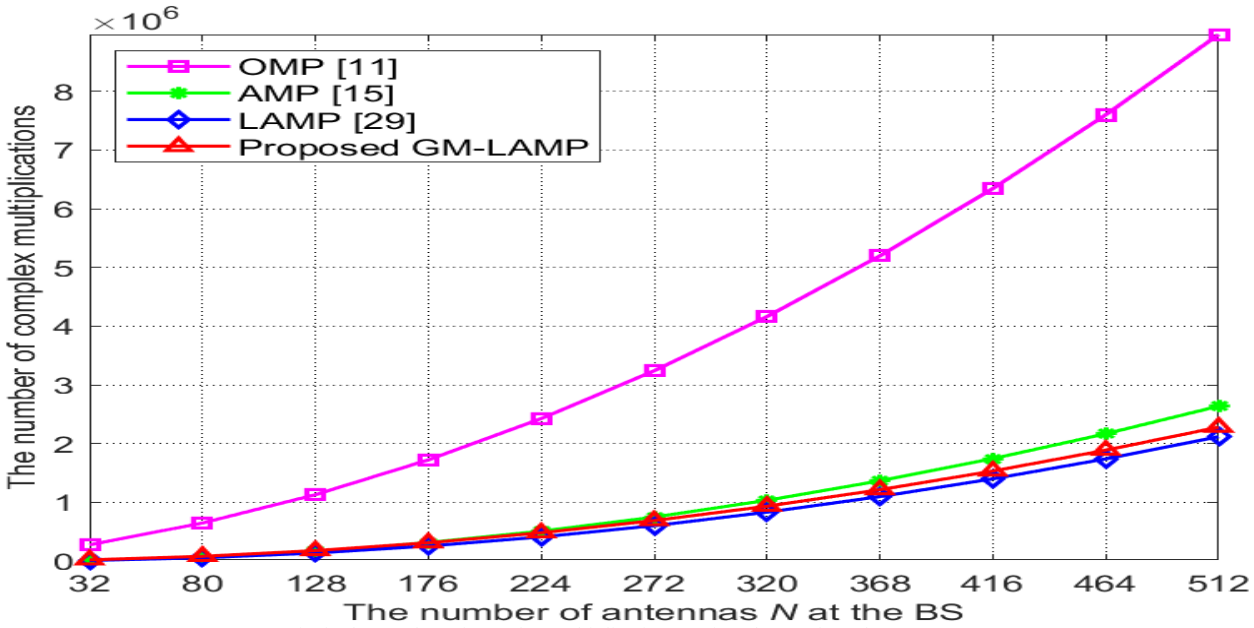

Fig f: The number of complex multiplications against the number of antennas N

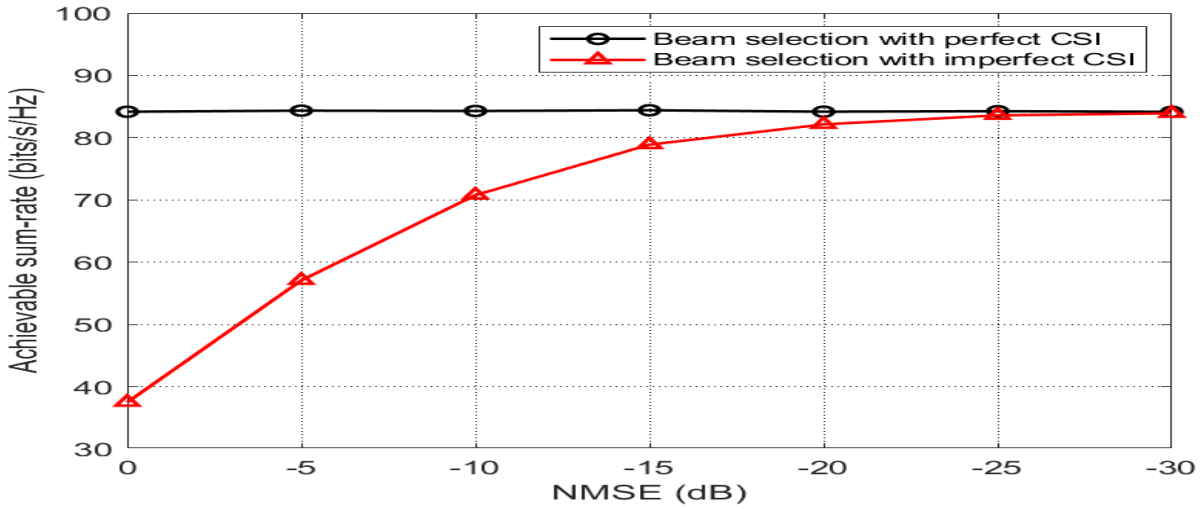

Fig: g Sum-rate for beam selection against different NMSE for the beamspace channel estimation.

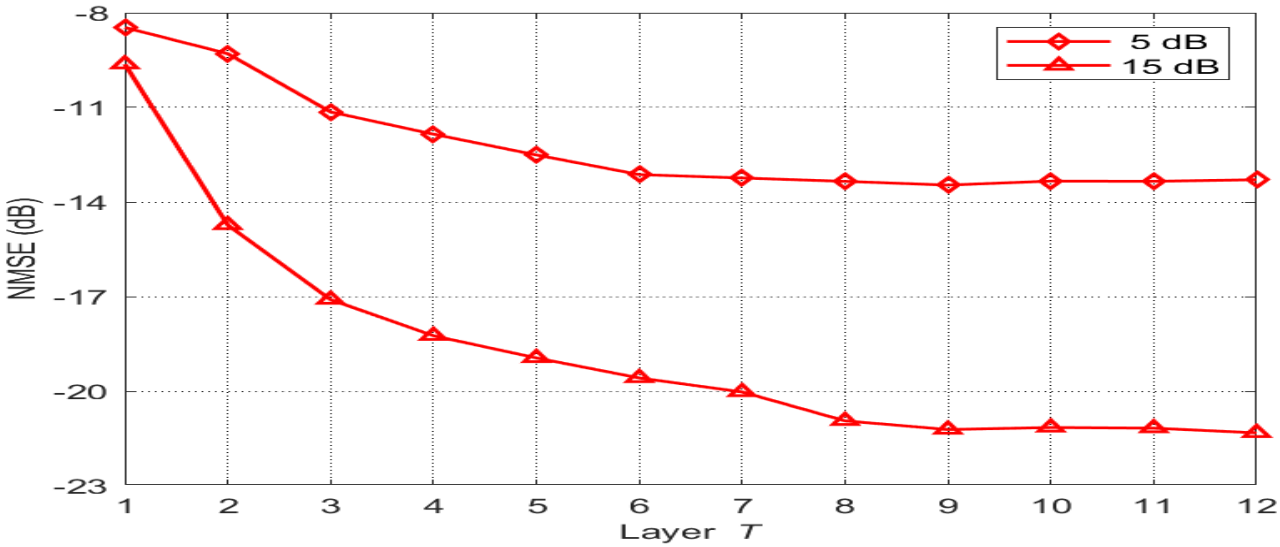

Fig. h NMSE performance against the number of layers for the GM-LAMP network.

COMPARISON ANALYSIS:

TABLE1 Comparison Table for SV Model(ULA)

SNR	NMSE	NMSE	NMSE	NMSE
	OMP	AMP	LAMP	GM_LAMP
0	-0.3089	-3.3919	-8.5239	**-9.1002**
5	-4.8021	-7.4161	-12.1955	**-13.5742**
10	-8.8331	-10.8537	-16.2185	**-16.7339**
15	-11.9175	-12.1955	-19.7701	**-20.780**
20	-13.7445	-14.9660	-21.7385	**-22.9176**

TABLE2: Comparison Table for SV Model(UPA)

SNR	NMSE	NMSE	NMSE	NMSE
	OMP	AMP	LAMP	GM_LAMP
0	0.2601	-2.6997	-7.6903	-8.5898
5	-3.5167	-5.9059	-11.0803	-12.7002
10	-6.2173	-8.1880	-14.7187	-15.2053
15	-7.7300	-9.5192	-18.1418	-18.6748
20	-8.4060	-10.1680	-20.1015	-20.4391

TABLE3: Comparison Table for Deep MIMO Dataset(ULA)

SNR	NMSE	NMSE	NMSE	NMSE
	OMP	AMP	LAMP	GM_LAMP
0	-0.4956	-3.6798	-12.7953	-13.1692
5	-5.1417	-7.9115	-17.3445	-18.8589
10	-9.5380	-11.7048	-20.8145	-21.5534
15	-13.4242	-14.8810	-25.5604	-26.5896
20	-16.2104	-17.1416	-29.0005	-29.4807

Table4: Comparison Table for Deep MIMO Dataset(UPA)

SNR	NMSE	NMSE	NMSE	NMSE
	OMP	AMP	LAMP	GM_LAMP
0	-0.0793	-3.2934	-11.8430	**-13.0985**
5	-4.2569	-7.0501	-16.1609	**-18.1398**
10	-7.9065	-10.1854	-19.5020	**-21.2844**
15	-10.5713	-12.6270	-23.9208	**-25.7664**
20	-12.0703	-14.2568	-27.0607	**-28.8282**

CONCLUSION:

Finally, this project proposed a prior-aided GM-LAMP network to solve the beamspace channel estimation problem in mmWave massive MIMO systems. Specifically, we first derive a new shrinkage function by exploiting the Gaussian mixture prior distribution of beamspace channel elements. Different from the original shrinkage function in the existing LAMP network, the derived Gaussian mixture shrinkage function can embody more prior information of the beamspace channel besides sparsity. Then, by integrating the LAMP network with the Gaussian mixture shrinkage function, a GM-LAMP based beamspace channel estimation scheme is developed. To verify the performance of our work, we provide simulation results on the Saleh-Valenzuela channel model and the ray-tracing based DeepMIMO dataset, respectively. Simulation results show that compared with the existing LAMP network and other conventional beamspace channel estimation schemes, the proposed GM-LAMP network considering the prior distribution can achieve better estimation accuracy with a low pilot overhead. We can find by leveraging the domain knowledge of the problems to be solved, the general DNN can be redesigned to improve the performance for the specific problems. For future work, we will follow the idea of the proposed GM-LAMP network to solve the channel estimation problem in terahertz (THz) communications by considering THz channel features

FUTURE SCOPE:

Today the cell framework requests higher information rates, low-inertness transmissions and sensors with ultra low-control utilization. Current cell frameworks of the fourth era (4G) are not ready to meet these developing requests of future versatile correspondence channels. To address this necessity, Generalized frequency division multiplexing (GFDM), a novel multi-bearer tweak system is proposed to fulfill the future needs of fifth era innovation. GFDM is a square based transmission strategy where beat molding is connected circularly to singular subcarriers. Dissimilar to customary orthogonal recurrence division multiplexing, GFDM transmits various images per subcarrier.

REFERENCES

[1] B. Muquet, Z. Wang, G. B. Giannakis, M. De Courville, and P. Duhamel, "Cyclic prefixing or zero padding for wireless multicarrier transmissions?" IEEE Trans. Commun., vol. 50, no. 12, pp. 2136– 2148, Dec. 2002.

[2] L. Hanzo, M. Munster, B. J. Choi, and T. Keller, OFDM and MC-CDMA for Broadband Multi-User Communications, WLANs, and Broadcasting. Chichester, U.K.: Wiley, 2003.

[3] L. Dai, Z. Wang, and Z. Yang, "Next-generation digital television terrestrial broadcasting systems: Key technologies and research trends," IEEE Commun. Mag., vol. 50, no. 6, pp. 150–158, Jun. 2012.

[4] J. Armstrong, "Analysis of new and existing methods of reducing intercarrier interference due to carrier frequency offset in OFDM," IEEE Trans. Commun., vol. 47, no. 3, pp. 365–369, Mar. 1999.

[5] H.-C. Wu, "Analysis and characterization of intercarrier and interblock interferences for wireless mobile OFDM systems," IEEE Trans. Broadcast., vol. 52, no. 2, pp. 203–210, Jun. 2006.

[6] B. Li et al., "MIMO-OFDM for high-rate underwater acoustic communications," IEEE J. Ocean. Eng., vol. 34, no. 4, pp. 634–644, Oct. 2009.

[7] Christo Ananth, Vivek.T, Selvakumar.S., Sakthi Kannan.S., Sankara Narayanan.D, "Impulse Noise Removal using Improved Particle Swarm Optimization", International Journal of Advanced Research in Electronics and Communication Engineering (IJARECE), Volume 3, Issue 4, April 2014,pp 366-370

[8] L. Dai, Z. Wang, J. Wang, and Z. Yang, "Joint time-frequency channel estimation for time domain synchronous OFDM systems," IEEE Trans. Broadcast., vol. 59, no. 1, pp. 168–173, Mar. 2013.

[9] W. Ding, F. Yang, C. Pan, L. Dai, and J. Song, "Compressive sensing based channel estimation for OFDM systems under long delay channels," IEEE Trans. Broadcast., vol. 60, no. 2, pp. 313–321, Jun. 2014.

[10] J. Chen, "Hybrid beamforming with discrete phase shifters for millimeterwave massive MIMO systems," IEEE Trans. Veh. Technol., vol. 66, no. 8, pp. 7604–7608, Aug. 2017. [11] S. Dutta, C. N. Barati, A. Dhananjay, D. A. Ramirez, J. F. Buckwalter, and S. Rangan, "A case for digital beamforming at mmWave," IEEE Trans. Wireless Commun., vol. 19, no. 2, pp. 756–770, Feb. 2020. [12] P. Skrimponis, S. Dutta, M. Mezzavilla,

S. Rangan, S. H. Mirfarshbafan, C. Studer, J. Buckwalter, and M. Rodwell, "Power consumption analysis for mobile mmwave and sub-THz receivers," in 2020 IEEE 6G Wireless Summit, Mar. 2020, pp. 1–5. [13] S. Jacobsson, G. Durisi, M. Coldrey, U. Gustavsson, and C. Studer, "Throughput analysis of massive MIMO uplink with low-resolution ADCs," IEEE Trans. Wireless Commun., vol. 16, no. 6, pp. 4038–4051, Jun. 2017. [14] Y. Li, C. Tao, G. Seco-Granados, A. Mezghani, A. L. Swindlehurst, and L. Liu, "Channel estimation and performance analysis of one-bit massive MIMO systems," IEEE Trans. Signal Process., vol. 65, no. 15, pp. 4075–4089, Aug. 2017. [15] J. Mo, P. Schniter, and R. W. Heath Jr., "Channel estimation in broadband millimeter wave MIMO systems with few-bit ADCs," IEEE Trans. Signal Process., vol. 66, no. 5, pp. 1141–1154, Mar. 2016. [16] T. S. Rappaport, R. W. Heath Jr., R. C. Daniels, and J. N. Murdock, Millimeter Wave Wireless Communications. Prentice Hall, 2015. [17] A. Alkhateeb, O. El Ayach, G. Leus, and R. W. Heath Jr., "Channel estimation and hybrid precoding for millimeter wave cellular systems," IEEE J. Sel. Topics Signal Process., vol. 8, no. 5, pp. 831–846, Oct. 2014. [18] J. Mo, P. Schniter, N. González Prelcic, and R. W. Heath Jr., "Channel estimation in millimeter wave MIMO systems with one-bit quantization," in Proc. Asilomar Conf. Signals, Syst., Comput., Pacific Grove, CA, USA, Nov. 2014, pp. 957–961. [19] P. Schniter and A. Sayeed, "Channel estimation and precoder design for millimeter-wave communications: The sparse way," in Proc. Asilomar Conf. Signals, Syst., Comput., Nov. 2014, pp. 273–277. [20] J. Deng, O. Tirkkonen, and C. Studer, "mmWave channel estimation via atomic norm minimization for multi-user hybrid precoding," in Proc. IEEE Wireless Commun. Netw. Conf. (WCNC), Apr. 2018, pp. 1–6. [21] Y. Wang, P. Xu, and Z. Tian, "Efficient channel estimation for massive MIMO systems via truncated two-dimensional atomic norm minimization," in Proc. IEEE Int. Conf. Commun. (ICC), May 2017, pp. 1–6. [22] J. Lee, G. Gil, and Y. H. Lee, "Channel estimation via orthogonal matching pursuit for hybrid MIMO systems in millimeter wave communications," IEEE Trans. Commun., vol. 64, no. 6, pp. 2370–2386, Jun. 2016. [23] P. Mächler, "VLSI architectures for compressive sensing and sparse signal recovery," Ph.D. dissertation, ETH Zürich, Switzerland, 2012. [24] C. Tsai, Y. Liu, and A. Wu, "Efficient compressive channel estimation for millimeter-wave large-scale antenna systems," IEEE Trans. Signal Process., vol. 66, no. 9, pp. 2414–2428, May 2018. [25] J. Brady, N. Behdad, and A. M. Sayeed, "Beamspace MIMO for millimeter-wave communications: System architecture, modeling, analysis, and measurements," IEEE Trans. Antennas Propag., vol. 61, no. 7, pp. 3814–3827, Jul. 2013. [26] G. Tang, B. N. Bhaskar, P. Shah, and B. Recht, "Compressed sensing off the grid," IEEE Trans. Inf. Theory, vol. 59, no. 11, pp. 7465–7490, Nov. 2013. [27] B. N. Bhaskar, G. Tang, and B. Recht, "Atomic norm denoising with applications to line spectral estimation," IEEE Trans. Signal Process., vol. 61, no. 23, pp. 5987–5999, Dec. 2013. [28] P. Zhang, L. Gan, S. Sun, and C. Ling, "Atomic norm denoising-based channel estimation for massive multiuser MIMO systems," in Proc. IEEE Int. Conf. Commun. (ICC), Jun. 2015, pp. 4564–4569. [29] B. Mamandipoor, D. Ramasamy, and U. Madhow, "Newtonized orthogonal matching pursuit: Frequency estimation over the continuum," IEEE Trans. Signal Process., vol. 64, no. 19, pp. 5066–5081, Oct. 2016. [30] F. Bellili, F. Sohrabi, and W. Yu, "Generalized approximate message passing for massive MIMO mmWave channel estimation with Laplacian prior," IEEE Trans. Commun., vol. 67, no. 5, pp. 3205–3219, May 2019. [31] C. Huang, L. Liu, C. Yuen, and S. Sun, "Iterative channel estimation using LSE and sparse message passing for mmWave MIMO systems," IEEE Trans. Signal Process., vol. 67, no. 1, pp. 245–259, Jan. 2019. [32] C. Jeon, O. Castañeda, and C. Studer, "A 354 Mb/s 0.37 mm2 151 mW 32-user 256-QAM near-MAP soft-input soft-output massive MU-MIMO data detector in 28nm CMOS," IEEE Solid-State Circuits Lett., vol. 2, no. 9, pp. 127–130, Sep. 2019. [33] C. Yeh, T. Chu, C. Chen, and C. Yang, "A hardware-scalable DSP architecture for beam selection in mm-Wave MU-MIMO systems," IEEE Trans. Circuits Syst. I, vol. 65, no. 11, pp. 3918–3928, Aug. 2018. [34] X. Liu, J. Sha, H. Xie, F. Gao, S. Jin, Z. Zhang, X. You, and C. Zhang, "Efficient channel estimator with angle-division multiple access," IEEE Trans. Circuits Syst. I, vol. 66, no. 2, pp. 708–718, Sep. 2018. [35] L. Somappa, S. Aeron, A. G. Menon, S. Sonkusale, A. A. Seshia, and M. S. Baghini, "On quantized analog compressive sensing methods for efficient resonator frequency estimation," IEEE Trans. Circuits Syst. I, pp. 1–10, Jun. 2020. [36] M. R. Akdeniz, Y. Liu, M. K. Samimi, S. Sun, S. Rangan, T. S. Rappaport, and E. Erkip, "Millimeter wave channel modeling and cellular capacity evaluation," IEEE J. Sel. Areas Commun., vol. 32, no. 6, pp. 1164–1179, Jun. 2014